 ISSN 2522-1841(Online)
ISSN 0005-2531 (Print)

SYNTHESIS AND INVESTIGATION OF SURFACE PROPERTIES OF SYSTEMS SiO_2-Gd_2O_3-Eu_2O_3

S.I.Niftaliev[1], I.V.Kuznetsova[1], Tran Nhat Anh[1]. F.M.Chyragov[2]
[1]Voronezh State University of Engineering Technologies, Voronezh, Russia
[2] *Baku State University, Baku, Azerbaijan*

ciraqov@mail.ru

Received 09.02.2026
Reviewed 28.03.2025
Accepted 30.04.2025

The ternary SiO_2-Gd_2O_3-Eu_2O_3 system was synthesized by TEOS hydrolysis in an aqueous medium via a sol–gel route. Thermal analysis showed that gel dehydration occurred mainly in the low-temperature region and was associated with the removal of physically adsorbed and weakly bound water. The apparent activation energy was 30–34 kJ/mol for the ternary gels and about 40 kJ/mol for the SiO_2 gel, indicating predominantly physical water binding. The calcined samples exhibited characteristic Eu^{3+} red emission, with the strongest band at 612 nm corresponding to the $^5D_0 \rightarrow {}^7F_2$ transition. The maximum luminescence intensity was obtained for the SiO_2-Gd_2O_3-Eu_2O_3 composition of 92:5:3 after calcination at 1000 °C, while further rare-earth oxide addition caused concentration quenching. The optimal excitation wavelength was 393 nm. The same 92:5:3 sample calcined at 700 °C showed the highest methylene blue adsorption capacity of 108.32 mg/g, which decreased to 79.08 mg/g after calcination at 1000 °C. These results show that the luminescence and adsorption properties of SiO_2-Gd_2O_3-Eu_2O_3 materials can be tuned by controlling the composition, calcination temperature, and acid–base state of the surface.

Keywords*: SiO_2-Gd_2O_3-Eu_2O_3 sol–gel synthesis; tetraethoxysilane; europium luminescence; methylene blue adsorption; acid–base surface properties*

https://doi.org/10.59849/0005-2531.2026.3.72

Introduction

The use of silica (SiO_2) as a host matrix for rare-earth ions has attracted considerable attention because of its chemical stability, thermal resistance, and suitability for luminescent material systems [1,2]. Owing to the presence of surface silanol groups and the possibility of incorporating metal ions into the silica network, SiO_2-based materials are widely used as carriers for optically active rare-earth ions [3].

The synthesis route and the silica source strongly affect the structure and optical properties of SiO_2–rare-earth systems. Various approaches have been used to prepare silicon oxide–metal oxide materials, including co-precipitation from solution, modification of pre-synthesized SiO_2 matrices with metal ions, and combined methods [4 - 6]. In particular, SiO_2-Gd_2O_3 ₂ and SiO_2-Eu_2O_3 materials have been synthesized using either silicon oxide isolated from kaolin followed by impregnation with rare-earth salt solutions, or co-precipitation from a TEOS solution containing Gd^{3+} and Eu^{3+} nitrates [4]. For Eu_2O_3–SiO_2 nanopowders, the transition intensity ratio $\eta = I(^5D_0 \rightarrow {}^7F_2) / I(^5D_0 \rightarrow {}^7F_1)$ was 1.25 for the kaolin-derived sample and 2.5 for the TEOS-derived sample, indicating that both the silica precursor and the synthesis method significantly influence the local environment of Eu^{3+} ions and, consequently, the luminescence behavior [4]. Eu^{3+} ions are widely used as luminescent centers and spectroscopic probes because their characteristic $^5D_0 \rightarrow {}^7F_j$ transitions are sensitive to the local symmetry of the surrounding environment. In Eu^{3+}-doped oxide and glass systems, intense red emission is commonly observed near 612–613 nm, corresponding to the hypersensitive electric-dipole transition $^5D_0 \rightarrow {}^7F_2$ [7]. For this reason, the combination

of Eu^{3+} and Gd^{3+} in silica-based matrices is of particular interest. Previous studies on silica xerogels and powders modified with Eu^{3+} and Gd^{3+} have shown direct excitation of Eu^{3+} at λ_{exc} = 393 nm through the $^7F_0 \rightarrow {}^5L_6$transition, as well as excitation features related to Gd^{3+} at λ_{exc} = 273 nm, corresponding to the $^8S_{7/2} \rightarrow {}^6I_j$ transitions [8–10]. However, the role of Gd^{3+} should be considered carefully, since enhancement of Eu^{3+} emission may arise not only from direct $Gd^{3+} \rightarrow Eu^{3+}$ energy transfer, but also from changes in the local environment and distribution of Eu^{3+} ions within the matrix [11].

The surface structure and chemical state of the oxide matrix are also closely related to the luminescence of rare-earth ions. In Eu^{3+}-doped SiO_2-Gd_2O_3 materials, adsorbed water and hydroxyl-containing species can act as non-radiative quenching centers, reducing the emission intensity of Eu^{3+} . Heat treatment can reduce these quenching centers and induce structural changes, thereby affecting the luminescent response of the material [12, 13].

In addition to optical properties, the acid–base characteristics of the surface are important for evaluating the behavior of luminescent oxide materials. The concentration and nature of surface active centers can correlate with the electro-optical properties of materials; for example, Brønsted basic centers may be related to the intensity of defect-related emission bands [14]. This indicates that surface chemistry can play an important role in determining both electro-optical and adsorption-related properties [15, 16].

There are many methods for determining the surface properties of substances: IR, X-ray, NMR spectroscopy, EPR, adsorption methods, etc [19, 20]. Among them, the indicator adsorption method is useful for evaluating acid–base centers on oxide surfaces. This method has been applied to SiO_2-Gd_2O_3-Eu_2O_3 powders obtained from solution, showing that specific adsorption increases with increasing pK_a of the indicators and rises sharply at pK_a = 9.4, confirming the presence of active basic centers [18].

Since these surface centers can also participate in the adsorption of organic molecules, methylene blue adsorption can be used as an additional probe of the surface activity of SiO_2containing materials. Mesoporous silicon dioxide samples exhibit good adsorption properties with respect to methylene blue dye, with a maximum adsorption capacity of 192 $mg \cdot g^{-1}$ [17, 21], demonstrating the importance of surface charge, porosity, and active adsorption sites in the interaction between SiO_2 -based materials and dye molecules [22, 23]. Thus, the combined analysis of acid–base properties and methylene blue adsorption provides complementary information about the surface state of the material.

Although binary SiO_2-Gd_2O_3 and SiO_2-Eu_2O_3 systems have been reported, they are limited in their ability to simultaneously combine the structural and surface functionality of silica, the red-emitting properties of Eu^{3+}, and the possible modifying effect of Gd^{3+} on the local environment and distribution of rare-earth ions. Therefore, the ternary SiO_2-Gd_2O_3-Eu_2O_3 system provides a suitable platform for tuning both optical and surface-related properties. Besides, the relationship between component concentration, heat treatment, surface acid–base properties, adsorption activity, and Eu^{3+} luminescence in this ternary system remains insufficiently clarified. Therefore, the aim of this work is to synthesize the SiO_2-Gd_2O_3-Eu_2O_3 system by a TEOS-based sol–gel route in an aqueous medium and to investigate the thermal behavior, surface acid–base properties, methylene blue adsorption activity, luminescence characteristics, and their interrelationship in the obtained materials.

Experimental part

Synthesis. For synthesis, 0.1 M solutions of $Gd(NO_3)_3 \cdot 6H_2O$ и $Eu(NO_3)_3 \cdot 6H_2O$ (chemically pure), tetraethoxysilane (98%) (chemically pure), and deionized water were used as starting components.

.

The SiO_2; SiO_2-Gd_2O_3-Eu_2O_3 systems were synthesized according to the block diagram shown in Fig.1

.

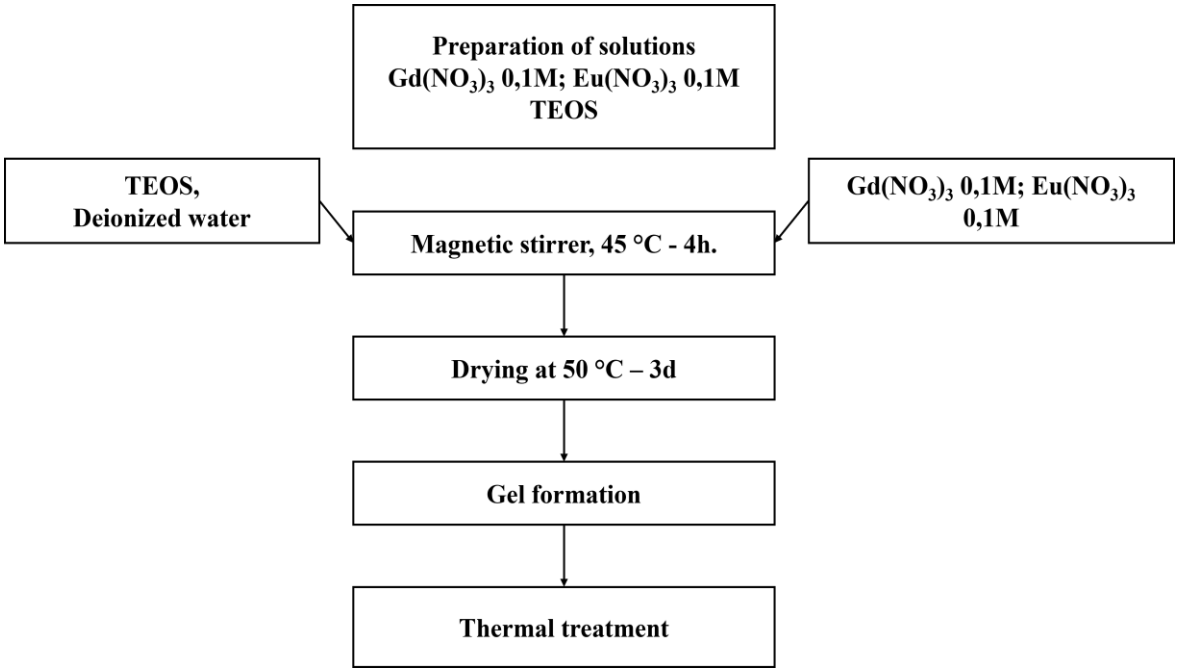

Fig.1.. Block diagram of the production and investigation of the SiO_2-Gd_2O_3-Eu_2O_3 system

The solutions were mixed together so that the ratio of silicon, gadolinium, and europium oxides was as follows [18]:

Samples	w, %
№ 1	100 % SiO_2 - 0 Gd_2O_3 – 0 Eu_2O_3
№ 2	95% SiO_2 - 3% Gd_2O_3 – 2% Eu_2O_3
№ 3	92% SiO_2 - 5% Gd_2O_3 – 3% Eu_2O_3
№ 4	90 % SiO_2 - 6 % Gd_2O_3 – 4 % Eu_2O_3

The prepared solutions were stirred on a magnetic stirrer combined with a thermostat at a temperature of 45°C for 4 hours, the pH of the solution before stirring was checked to be around 6-7. The rotation speed of the magnetic stirrer was kept constant in all experiments. The mixtures obtained after stirring were dried at 50°C for 3 days. After gel formation, the samples were subjected to thermal analysis. The thermodestruction processes were studied using thermogravimetry (TG) and differential scanning calorimetry (DSC) methods on "NETZSCH STA 449 F3 Jupiter" simultaneous thermal analyzer. The samples were placed in platinum crucibles and heated in a nitrogen atmosphere from 20°C to 500°C at a rate of 5°C/min [24].

Characterization.

To study the adsorption capacity for methylene blue (MB), acid-base properties, and luminescence, gel samples were annealed at temperatures of 700 °C and 1000 °C for 4 hours in a muffle furnace. The adsorption value was determined by spectrophotometric measurement of the decrease in MB dye concentration in the solution after reaching adsorption equilibrium [25]. MB solution with an initial concentration of 150 mg/dm³ was prepared, to construct a calibration curve by dilution, 10 solutions with concentrations of 0.75–13.50 mg/dm³ were obtained. The sample weights were placed in a conical flask, 25 cm³ of indicator solution was

added, mixed, and centrifuged. One cm³ of the clarified solution was taken and the optical density was measured at a wavelength of 400 nm. The adsorption activity X (mg/g) was calculated using the formula:

$$X = \frac{(C_1 - C_2 \cdot K) \cdot 0.025}{m}$$

where C_1 - the concentration of the initial indicator solution, mg/dm^3; C_2 - the concentration of the solution after contact with the sample, mg/dm^3; **K** - the dilution factor of the solution; **0,025** - the volume of the indicator solution, dm^3; **m** - the mass of the sample, g.

To study the distribution of surface centers according to their acid-base properties, the Hammett method was used with six indicators with pK_a values ranging from +0.80 to +12.80 [26]. The solutions under study were examined in 1 mm thick cuvettes relative to distilled water on a "KFK-2MP" photocolorimeter at a wavelength corresponding to the absorption maximum of each indicator (Table 3).

$$g = \frac{c.V}{D_o} \cdot \left| \frac{|D_o - D_1|}{a_1} \pm \frac{|D_o - D_2|}{a_2} \right|$$

where **c** - the indicator concentration, mol/dm^3; **V** - the sample volume, dm^3; D_0 - the optical density of the initial indicator; D_1 - the optical density of the indicator after sorption by the sample; D_2 - the optical density of the blank sample (solvent + material sample); a_1, a_2 - the sample weights, g.

An Ocean Optics 2000+ spectrophotometer was used to measure luminescence spectra in the range of 200–900 nm (the spectrometer's sensitivity range is from 200 to 1000 nm). and the oscillations were excited using a semiconductor laser with a wavelength of 405 nm.

Results and discussion

During the synthesis of samples using the method shown in Figure 1, silicic acids are obtained as a result of TEOS hydrolysis according to equation (1), followed by adsorption of metal ions on the surface of silicic acid (2). Next, silanols bind to each other, forming a bond ≡ Si – O – Si ≡ with the release of water and alcohol (3), (4); metal ions are incorporated into the siloxane skeleton (5), leading to the formation of dimers, trimers, and larger SiO_2 polymers [18].

$(C_2H_5O)_3 \equiv Si - (OC_2H_5) + H_2O \rightarrow Si(OH)_4 + 4\ C_2H_5OH$ (1);

$Eu^{3+} \rightarrow Si(OH)_4 \leftarrow Gd^{3+}$ (2);

$\equiv Si - (OH) + (HO) - Si \equiv \rightarrow \equiv Si - O - Si \equiv + H_2O$ (3);

$\equiv Si - (OC_2H_5) + (HO) - Si \equiv \rightarrow \equiv Si - O - Si \equiv + C_2H_5OH$ (4);

$\equiv Si - O - Si \equiv + Me^{n+} \rightarrow \equiv Si - O - - - Me - Si \equiv$ (5).

Silicon particles and silicon polymers suspended in a solvent will crosslink, forming a network, facilitating a transition from a liquid to a solid state, leading to the formation of gels.

The thermal degradation process of the gel was studied using synchronous thermal analysis (Fig. 2, 3).

The thermal behavior of the gel was investigated by synchronous thermal analysis (Figs. 2, 3). A major mass loss of 88–93% was observed in the temperature range of 30–119 °C (TG curve) (Fig. 3, Table 1). Such a high mass loss is characteristic of gel-derived materials and can be attributed mainly to the removal of physically adsorbed and weakly bound water [19].The degree of conversion, α, was calculated from the TG curves in the temperature range of 30–135 °C using the expression

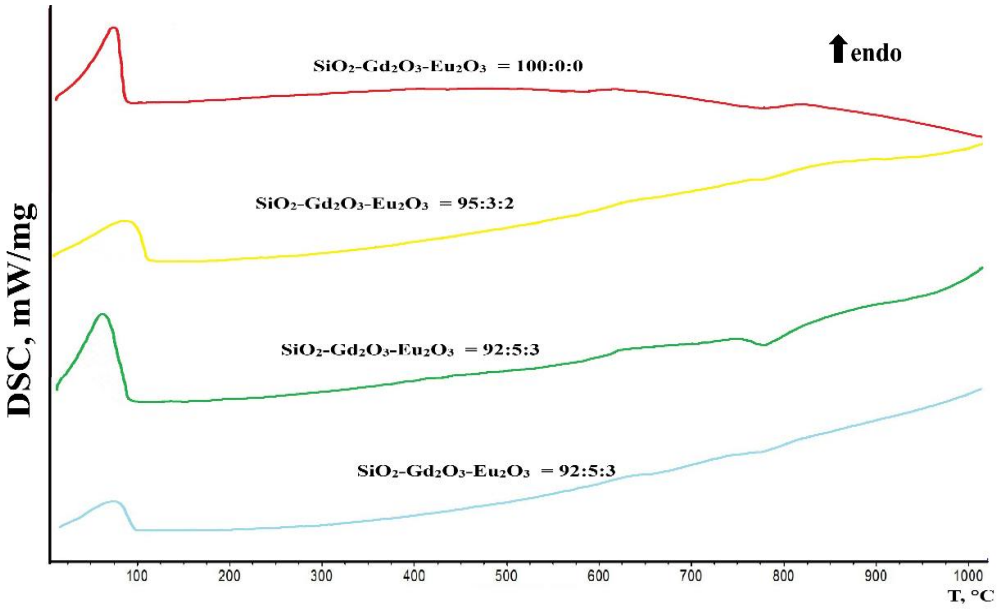

Fig.2. DSC curves during heating of the SiO_2-Gd_2O_3-Eu_2O_3 system with different ratios

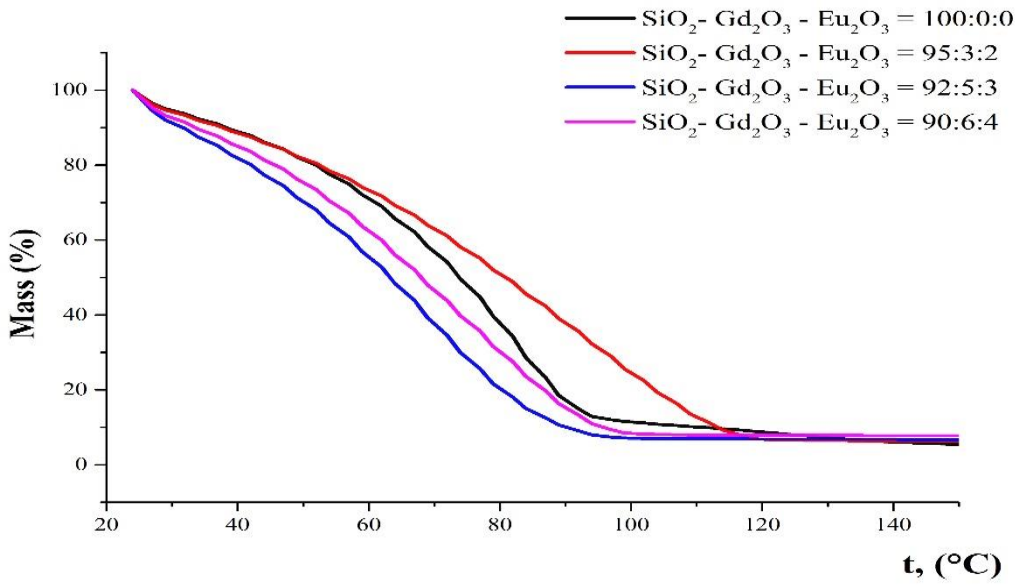

Fig.3. TG curves for heating the SiO_2-Gd_2O_3-Eu_2O_3 system with different ratios

Table 1. Results of gel analysis using the thermal method

Samples SiO_2-Gd_2O_3-Eu_2O_3	Temperature peak, °C; thermal effect, J/g	Total weight loss, %	Dehydration reaction activation energy, E_a, kJ/mol
100:0:0	Complex peak: 46,6 – 97,7°C, peak 85,8°C; 1277 J/g	88,11	40.00
95:3:2	Complex peak:: 30 – 123 °C, peak 102,7°C; 1771 J/g	93,39	30.13
92:5:3	Complex peak:: 36,1 – 101°C; peak 72,3 °C; 1255 J/g	92,89	32.33
90:6:4	Complex peak:: 46-103,7 °C; peak 85,9 °C; 1258 J/g	91,83	34.44

$$\alpha = \frac{\Delta m_i}{\Delta m_{omax}}$$

where Δm_i is the mass loss at a given temperature and Δm_{max} is the total mass loss of the process.

The α–T curve exhibits an S-shaped profile, indicating that water removal proceeds continuously with increasing temperature rather than through several clearly separated mass-loss steps (Fig. 4). This process can be described as a transformation of the type A(solid) → B(solid) + C(gas), in which water is released from the solid phase.

The rate of the process was considered to depend on both temperature and degree of conversion and can be written in the general form:

$$\frac{d\alpha}{d\tau} = \omega(T) f(\alpha)$$

where α is the degree of conversion and τ is time.

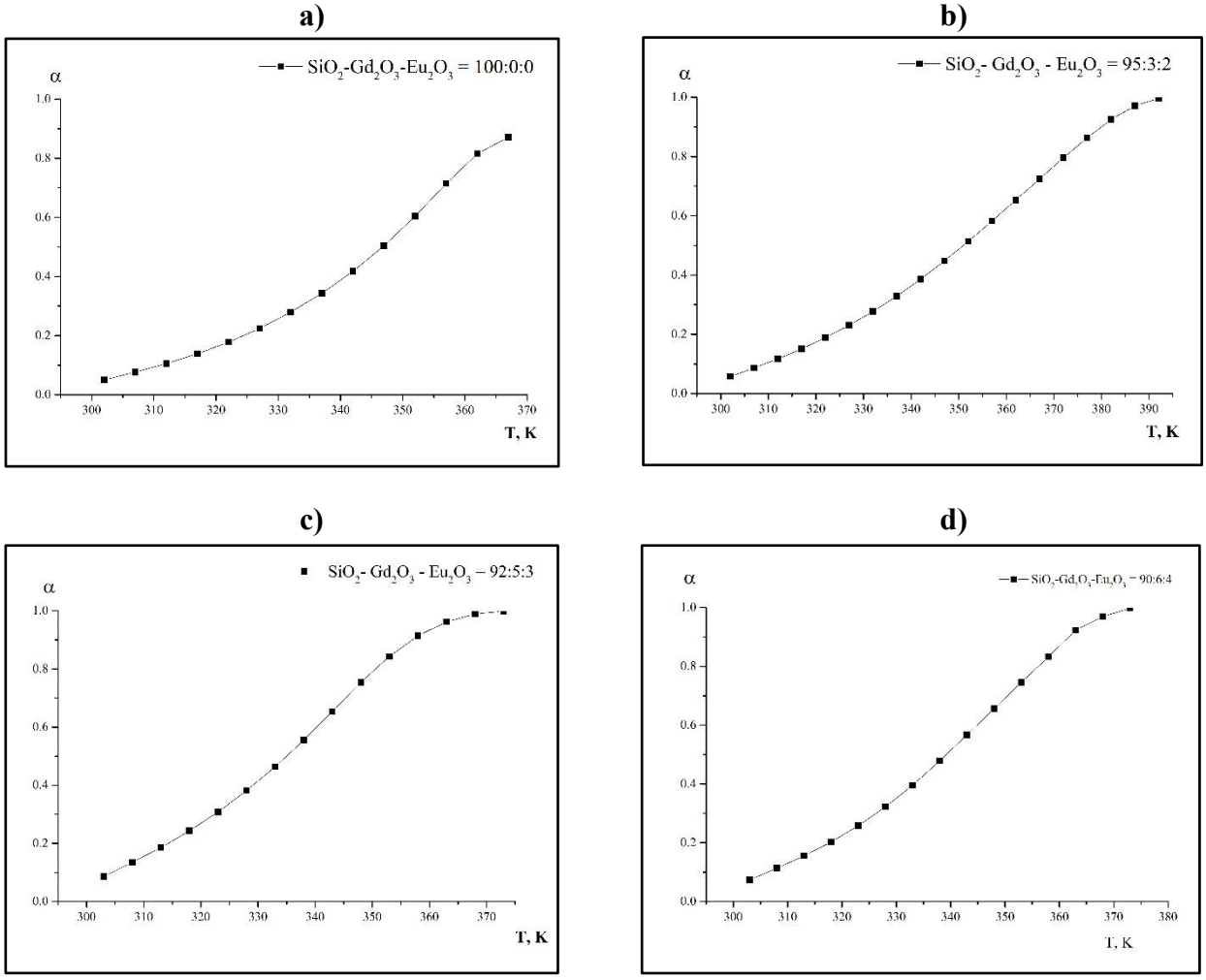

Fig.4. Dependence of the degree of conversion α on T during dehydration of the SiO_2-Gd_2O_3-Eu_2O_3 gel system with ratios: a) 100:0:0, b) 95:3:2, c) 92:5:3, d) 90:6:4

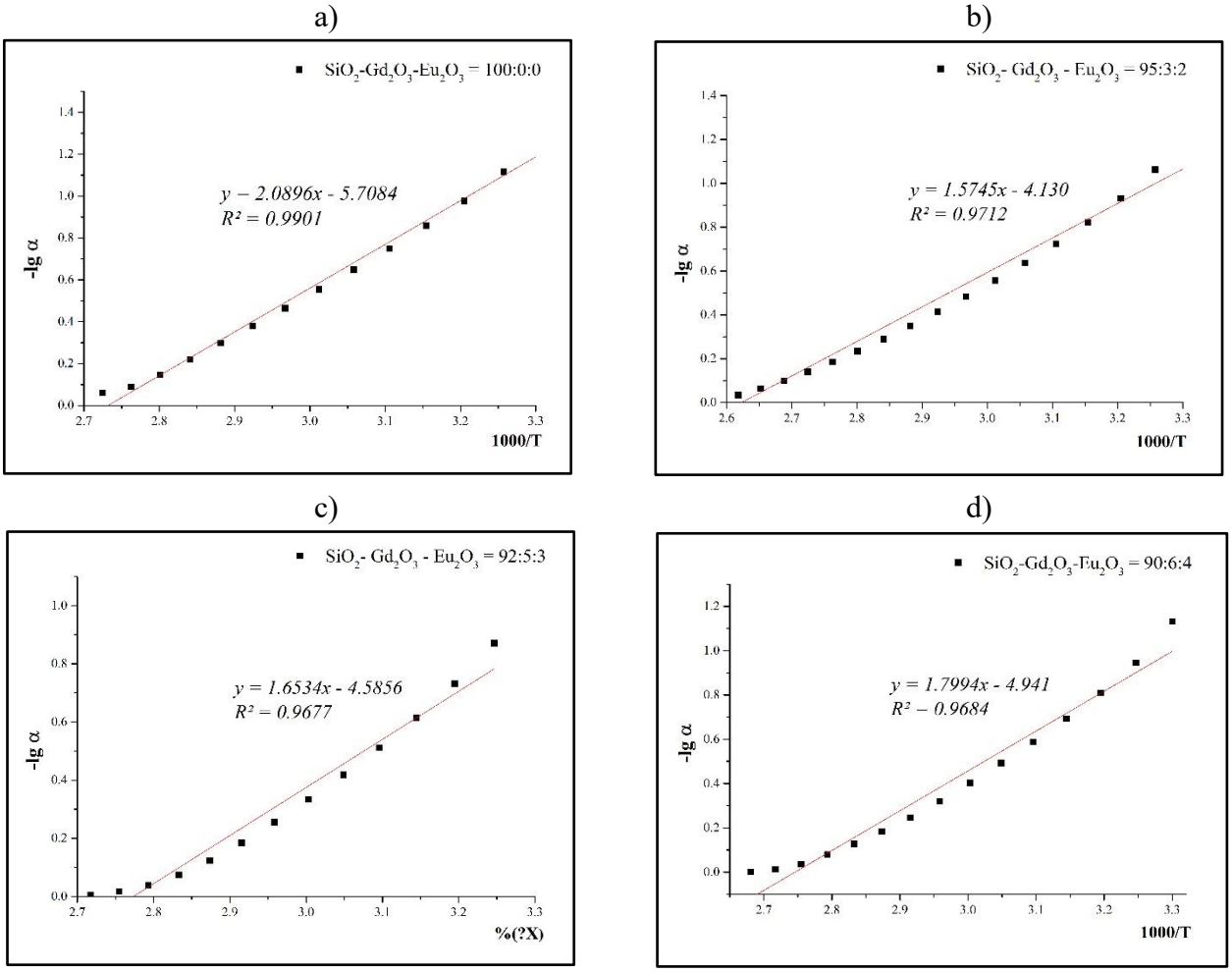

Fig.5 Dependence of –lgα on 1000/T during dehydration of the SiO_2-Gd_2O_3-Eu_2O_3 gel system with ratios: a) 100:0:0, b) 95:3:2, c) 92:5:3, d) 90:6:4

The temperature dependence of the rate constant was described by the Arrhenius equation:

$$w(T) = A \exp(-\frac{E_a}{RT})$$

where A is the pre-exponential factor and Ea is the activation energy.

In the present study, the dehydration process was approximated by a first-order kinetic model. This model was used as an apparent description of the main dehydration step rather than as proof of a unique reaction mechanism. For kinetic treatment, the experimental data were linearized by plotting (–lgα) versus (1000/T) (Fig. 5).

The linearized plots show a high degree of linearity ($R^2 > 0.96$), supporting the use of this approximation within the selected temperature range. The activation energy was determined from the slope of the linear section according to the Arrhenius relationship.

The activation energy obtained for dehydration was 30–40 kJ/mol. This relatively low value indicates that the mass loss is mainly associated with the removal of water species weakly interacting with the silica-based matrix. In gel systems, such behavior is characteristic of dehydration/desorption processes. Water molecules may interact with the silica matrix to different extents, mainly through physical

adsorption and hydrogen-bonding interactions with surface hydroxyl groups. Therefore, the large mass loss observed in this work can be attributed to the combined removal of adsorbed water species with different binding strengths. This interpretation is more consistent with dehydration/desorption than with structural decomposition of the siloxane framework. In [3] the authors also showed that the desorption energy of water is 26–44 kJ/mol, which corresponds to the physical adsorption of water. In [27] the authors obtained that the activation energy (E_a ~ 45 kJ/mol) and desorption heat (ΔQ ~ 46 kJ/mol) are practically identical. Therefore, the value of ~45 kJ/mol is consistent with the energy required to break approximately two hydrogen bonds per water molecule, which is typical for strong physical adsorption on silicon surfaces containing –OH groups.

When excited by UV light with a wavelength of 405 nm, samples of the system annealed at 700 °C and 1000 °C emitted red light (Figs. 6, 7). We observe five main emission peaks: 578 nm ($^5D_0 \rightarrow {}^7F_0$ transition), 590 nm ($^5D_0 \rightarrow {}^7F_1$ transition), 612 nm ($^5D_0 \rightarrow {}^7F_2$ transition), 649 nm ($^5D_0 \rightarrow {}^7F_3$ transition), and 697 nm ($^5D_0 \rightarrow {}^7F_4$ transition). When Eu^{3+} ions are excited, electrons transition to higher energy levels and then relax without emission to a stable peak level of $^5D_0$. From $^5D_0$, electrons return to the ^7F_J level (J=0,1,2,3,4) and red light is emitted.

It can be seen that for all samples, the most pronounced emission peak is at 612 nm with a $^5D_0 \rightarrow {}^7F_2$ transition. The $^5D_0 \rightarrow {}^7F_1$ transition is magneto dipole, the intensity of which practically does not depend on the substrate and the environment. In contrast, the $^5D_0 \rightarrow {}^7F_2$ transition is electric dipole, which has increased sensitivity, and its intensity strongly depends on the local environment: it is activated in low-symmetry structures and suppressed in more symmetric environments [7].

The luminescence intensity of all samples calcined at 1000 °C was significantly higher than that of the samples calcined at 700 °C, which is consistent with previous reports [28]. This enhancement can be attributed not only to the reduction of surface-related luminescence quenching centers but also to changes in the local environment around Eu^{3+} ions.

These surface centers are schematically illustrated in Fig. 9. In the SiO_2-Gd_2O_3-Eu_2O_3 system, Eu^{3+} ions act as the main red-emitting centers, residual surface hydroxyl groups, such as ≡Si–OH and =Si(OH)₂, are likely to act as non-radiative quenching centers owing to high-energy O–H vibrations. In addition, defect-related deprotonated oxygen species, such as $–O^–$ groups, may also contribute to non-radiative relaxation pathways.. With increasing calcination temperature, the concentration of these quenching centers decreases, thereby enhancing Eu^{3+} emission.

The transition intensity ratio $\eta = I(^5D_0 \rightarrow {}^7F_2)/I(^5D_0 \rightarrow {}^7F_1)$ was used to evaluate the monochromaticity and local symmetry of Eu^{3+} emission. High color purity is characterized by a large η value. In this study, η was higher than 4 for most samples and reached 4.5 for the 92:5:3 sample, which is higher than that reported for the binary SiO_2-Eu_2O_3 ₃ system [4]. This result indicates high color purity and a highly asymmetric coordination environment around Eu^{3+} ions, as reflected by the dominance of the hypersensitive electric-dipole transition $^5D_0 \rightarrow {}^7F_2$ over the magnetic-dipole transition $^5D_0 \rightarrow {}^7F_1$. Therefore, the enhanced Eu^{3+} emission may be mainly associated with changes in the local environment and distribution of Eu^{3+} ions caused by the presence of Gd^{3+}. In addition, although the PLE spectrum does not provide clear evidence of efficient $Gd^{3+} \rightarrow Eu^{3+}$ energy transfer in the high-energy region, possible contributions from indirect or less efficient energy-transfer pathways between rare-earth ions cannot be completely excluded [30,31].

The ratio of the system components affects the emissivity of the sample. It can be seen that the radiation intensity increases with an increase in the ratio of Gd and Eu components and is associated with an increased number of luminescence centers. At 700 °C the highest radiation intensity is observed in sample 4 (SiO_2-Gd_2O_3-Eu_2O_3 – 90:6:4), with the maximum europium content. After annealing at 1000 °C, the highest radiation intensity was observed in sample 3 (SiO_2-Gd_2O_3-Eu_2O_3 – 92:5:3). With a further increase of the Gd and Eu ratio, the radiation intensity decreased, which may be due to the interaction between Eu^{3+} ions and luminescence quenching [29]

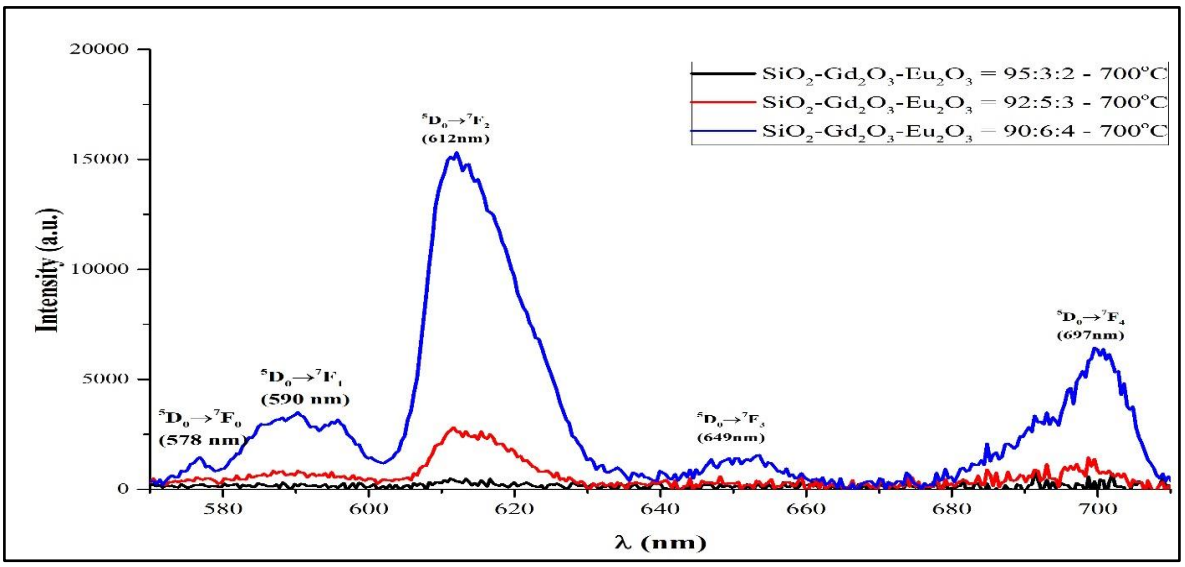

.

Fig.6. Emission spectra for SiO_2-Gd_2O_3-Eu_2O_3 systems of various compositions, pre-calcined at 700 °C: a) 95:3:2, b) 92:5:3, c) 90:6:4

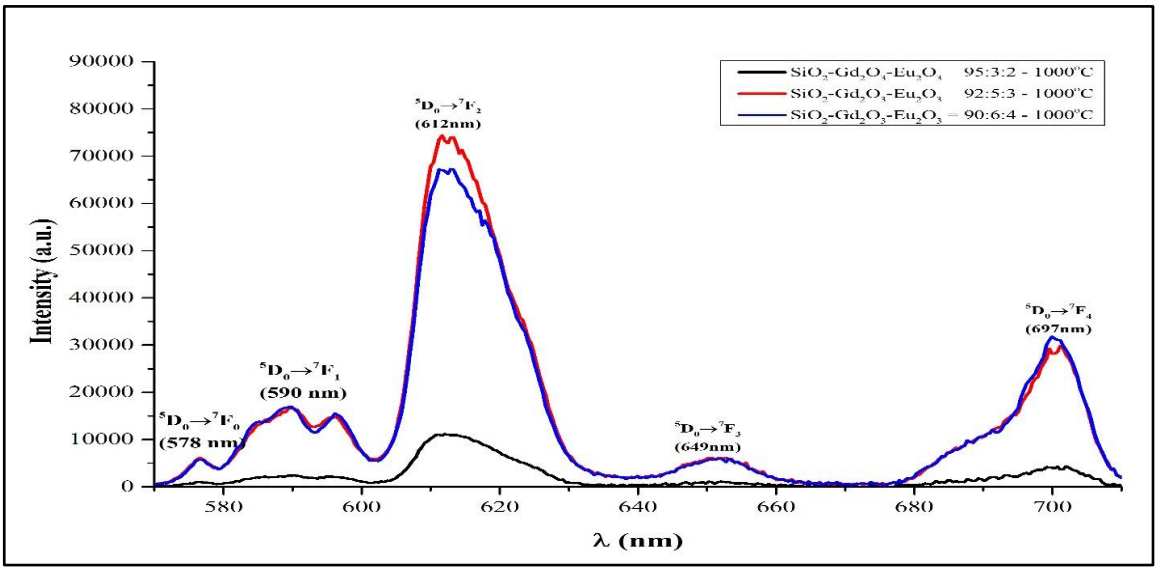

Fig.7. Emission spectra for SiO_2-Gd_2O_3-Eu_2O_3 systems of various compositions, pre-calcined at 1000 °C: a) 95:3:2, b) 92:5:3, c) 90:6:4

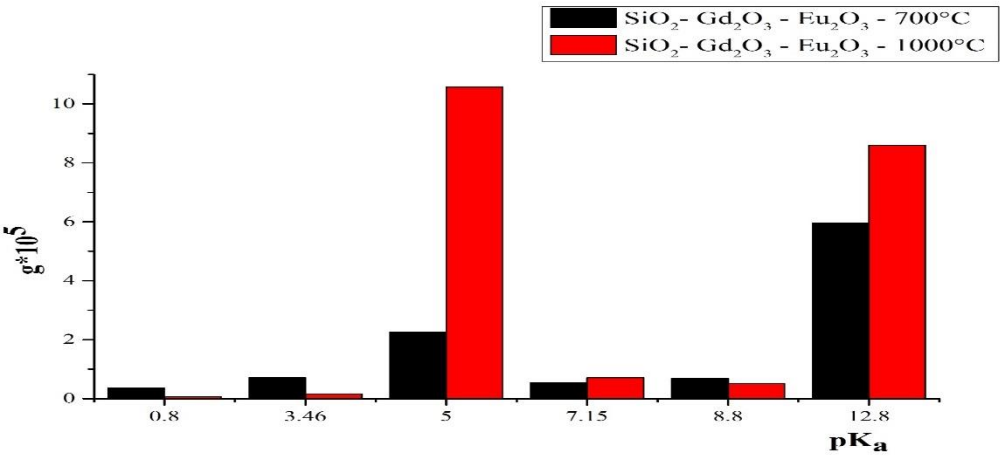

Fig8. Results of determining the specific adsorption of SiO_2-Gd_2O_3-Eu_2O_3 samples with a composition of 92:5:3, pre-calcined at 700 and 1000 °C

Table 2. Results of determining the specific adsorption of SiO_2-Gd_2O_3-Eu_2O_3 composition 92:5:3, precalcined at 700 and 1000 °C

Indicator	pK_a	Wavelength of maximum absorption λ, nm	Specific adsorption of the system,, g × 10^5, mol/g	
			SiO_2-Gd_2O_3-Eu_2O_3 (700 °C)	SiO_2-Gd_2O_3-Eu_2O_3 (1000 °C)
Crystal violet	+0,8	580	0.36	0.064
Methyl orange	+3,46	460	0.70	0.16
Methyl red	+5,0	430	2.25	10.57
P – Nitrophenol	+7,15	360	0.55	0.70
Thymol blue	+8,8	430	0.68	0.51
Indigo carmine	+12,8	610	5.95	8.60

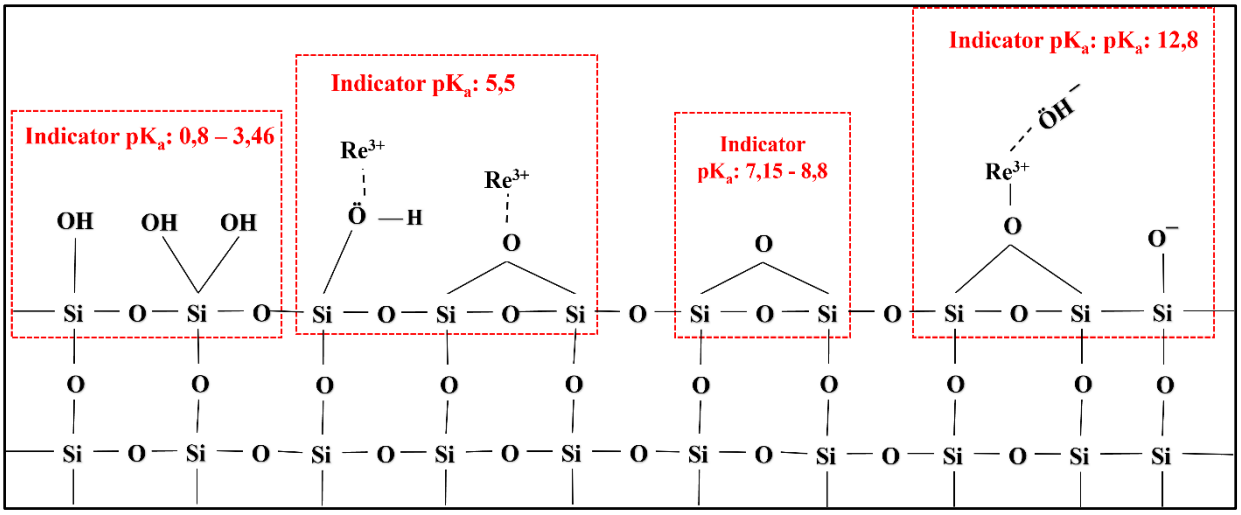

Fig.9. Schematic diagram of the surface of the SiO_2-Gd_2O_3-Eu_2O_3 system

Since the emission band at 612 nm is the most intense in the photoluminescence spectra (Figs. 6, 7), the excitation spectrum was recorded by monitoring the red emission at 612 nm, corresponding to the $^5D_0 \rightarrow {}^7F_2$transition of Eu^{3+}. The photoluminescence excitation (PLE) spectrum of the SiO_2-Gd_2O_3-Eu_2O_3 system was measured in the 350–550 nm range and is shown in Fig. 10.

The observed narrow excitation bands are assigned to intraconfigurational 4f–4f transitions of Eu^{3+} from the $^7F_0$ ground state to the excited states $^5D_4$ (362 nm), $^5G_j/^5L_7$ (371–390 nm), $^5L_6$ (393 nm), $^5D_3$ (416 nm), $^5D_2$ (465 nm), and $^5D_1$ (525 nm) [29]. Among these transitions, the band at 393 nm, corresponding to the $^7F_0 \rightarrow {}^5L_6$ transition, exhibits the highest excitation efficiency for generating the 612 nm red emission. This transition is known as one of the strongest direct excitation channels of Eu^{3+} in the near-UV region [7,32]. Therefore, the selection of 393 nm as the excitation wavelength is supported not only by the maximum intensity observed in the PLE spectrum, but also by the spectroscopic nature of the Eu^{3+} $^7F_0 \rightarrow {}^5L_6$ transition.

.

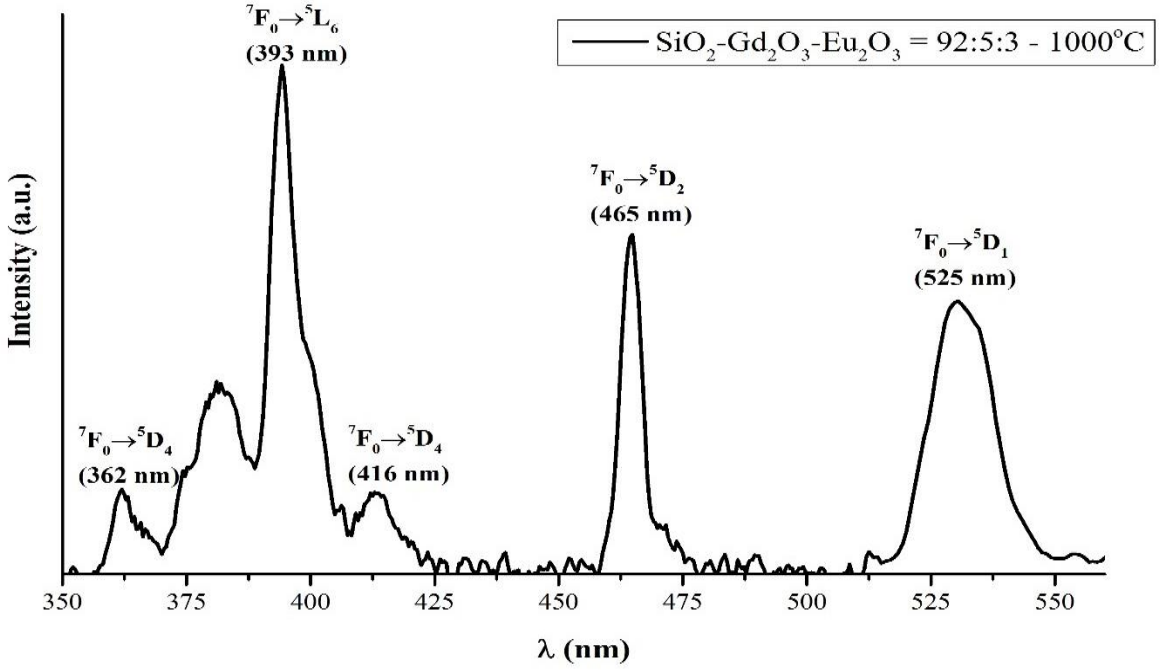

Fig.10. Excitation spectra of the SiO_2-Gd_2O_3-Eu_2O_3 system was monitored by the red emission at λ_{em} = 612 nm.

In contrast, the excitation bands at 362, 416, 465, and 525 nm are less intense under the same monitoring conditions, indicating that these excitation pathways are less efficient in populating the emitting $^5D_0$ level in the present system. Thus, 393 nm can be considered the optimal excitation wavelength for Eu^{3+} red emission at 612 nm under the investigated experimental conditions.Sample 3 (SiO_2-Gd_2O_3-Eu_2O_3 with a content of 92:5:3) was used to study the acid-base properties of the surface and its ability to adsorb MB. According to preliminary data [18], the activation energy of the hydrolysis reaction during the synthesis of this sample has a minimum value, which means that the hydrolysis reaction rate during the formation of this ternary system is maximum, and obtaining material of this composition in industrial quantities is less energy-intensive.

The distribution of indicator adsorption centers on the surface of the studied systems showed several characteristic regions, among which weakly acidic and strongly basic/donor centers were predominant. These centers were identified using indicators with pK_a values of approximately 5.0 and 12.8, respectively (Fig. 8, Table 2). The region corresponding to strongly acidic/Brønsted acidic centers is associated with surface hydroxyl groups, primarily isolated silanol groups (≡Si–OH) and geminal silanol groups (=$Si(OH)_2$), located on the silica surface and structural defects. The relatively low contribution of this region, especially after high-temperature calcination, indicates a decrease in the amount of free hydroxyl-containing Brønsted sites. This can be attributed to dehydroxylation and condensation of neighboring silanol groups with the formation of siloxane bonds (3).Thus, calcination promotes the removal or partial blocking of free ≡Si–OH and =$Si(OH)_2$ groups, reducing the concentration of strong Brønsted acidic centers on the surface.

The weakly acidic region is likely associated with rare-earth-containing surface sites involving Eu^{3+} and Gd^{3+} ions (2),(5) [35]. Due to their high positive charge and vacant orbitals, these ions may act as weak Lewis acidic centers and polarize neighboring silanol groups. Partial shielding of free Brønsted silanol sites by rare-earth ions may also contribute to the redistribution of acidic centers toward the weakly acidic region. The stronger contribution of this region after calcination at 1000 °C can be attributed to surface restructuring and improved accessibility of Eu^{3+}/Gd^{3+}-related Lewis acidic sites, despite the simultaneous decrease in free silanol groups. The high adsorption intensity in the pK_a = 12.8 region indicates the presence of strong basic/donor centers. Following the interpretation proposed in [5], metal ions on the silica surface can facilitate the sorption of OH^- ions, thereby enhancing the electron-donating properties of the surface. Accordingly, the strong adsorption at pK_a = 12.8 may be related to rare-earth-containing surface sites, sorbed hydroxide ions, hydroxyl groups, and electron-rich oxygen species. Overall, the change in the distribution of adsorption centers with calcination temperature reflects the combined effects of dehydroxylation, surface reconstruction, partial blocking of Brønsted silanol sites, and exposure of rare-earth-containing active sites.

For the SiO_2-Gd_2O_3-Eu_2O_3 sample (calcined at 700 °C), the adsorption activity according to MB per 1 g of product – 108.32 mg/g. In the SiO_2-Gd_2O_3-Eu_2O_3 sample (calcined at 1000 °C), the adsorption activity is lower – 79.08 mg/g. The sorption capacity according to MB can be determined by the content of micropores with a width of 1.06–1.95 nm and mesopores with a width of 2.00–2.24 nm in the structure of sorbents [33]. In addition to structural parameters, the chemical composition of the adsorbent surface also affects the adsorption value. Thus, MB, being a cationic dye, will interact with negatively charged centers on the adsorbent surface, which will lead to increased adsorption. The acid center creates a local positive charge or an electron deficit region. This area repels MB cations and prevents MB adsorption [34], which means that in the SiO_2-Gd_2O_3-Eu_2O_3 system, there is an excess of negatively charged centers on the surface, which is consistent with the results of the study of the acid-base properties of the surface presented above.

Conclusions

The SiO_2-Gd_2O_3-Eu_2O_3 ternary system was successfully synthesized by TEOS hydrolysis in an aqueous medium. Thermal analysis showed that the main mass loss of the gels occurs in the low-temperature region and is associated with the removal of physically adsorbed and weakly bound water. The results demonstrate that heat treatment plays a key role in controlling both the surface state and luminescence behavior of the materials. Calcination changes the acid–base state of the surface, reduces hydroxyl-related quenching

centers, and may promote structural rearrangement of the oxide matrix, which facilitates a more favorable local environment for Eu^{3+} ions, thereby enhancing Eu^{3+} emission. The samples exhibited characteristic Eu^{3+} red emission dominated by the $^5D_0 \rightarrow {}^7F_2$ transition at 612 nm, while the 393 nm band, corresponding to the $^7F_0 \rightarrow {}^5L_6$ transition, was the most effective excitation channel. The high $\eta = I(^5D_0 \rightarrow {}^7F_2)/I^5D_0 \rightarrow {}^7F_1)$ values indicate a highly asymmetric local environment around Eu^{3+} ions, which may be associated with the modifying effect of Gd^{3+} in the silica matrix. At the same time, higher-temperature calcination increased the relative contribution of acidic surface centers, leading to a decrease in methylene blue adsorption capacity. The composition SiO_2-Gd_2O_3-Eu_2O_3 = 92:5:3 showed the most favorable balance between luminescence performance and adsorption activity. Overall, the functional properties of this ternary oxide system can be tuned through the component ratio and calcination temperature, confirming its potential as a multifunctional material combining Eu^{3+} luminescence with surface adsorption functionality.

References

1. Baranovskaya V.B., Karpov Yu.A., Petrova K.V. et al. Topical trends in the application of rare-earth metals and their compounds in the production of magnetic and luminescent materials. Izvestiya. Tsvetnaya Metallurgiya 2020. № 6. P. 4–23. doi.org/10.17073/0021-3438-2020-6-4-23[in Russian].
2. Moretti E., Talon A., Storaro L. et al. Concentration quenching and photostability in Eu(dbm)₃phen embedded in mesoporous silica nanoparticles. J. Lumin. 2014. V. 146. P. 178–185. doi.org/10.1016/j.jlumin.2013.09.059
3. Zhuravlev L.T. The surface chemistry of amorphous silica. Zhuravlev model. Colloids Surf. A: Physicochem. Eng. Aspects. 2000. V. 173. № 1–3. P. 1–38. doi.org/10.1016/S0927-7757(00)00556-2
4. Niftaliev S.I., Kuznetsova I.V., Zvereva I.A. et al. Silicon oxide modified with gadolinium and europium oxides—synthesis, properties and application prospects. Glass Phys. Chem. 2023. V. 49. P. 150–159. doi.org/10.1134/S108765962260096X
5. Niftaliev S.I., Kuznetsova I.V., Lygina L.V. et al. Synthesis and study of La_2O_3–SiO_2 systems obtained from kaolin and tetraetoxysilane. Glass Phys. Chem. 2024. V. 50. P. 411–417. doi.org/10.1134/S1087659624600959
6. Secu M., Secu C., Bartha C. Optical properties of transparent rare-earth doped sol-gel derived nano-glass ceramics. Materials. 2021. V. 14. Article 6871. doi.org/10.3390/ma14226871
7. Binnemans K. Interpretation of europium(III) spectra. Coord. Chem. Rev. 2015. V. 295. P. 1–45. doi.org/10.1016/j.ccr.2015.02.015
8. Szpikowska-Sroka B., Żądło M., Czoik R. et al. Energy transfer from Gd^{3+} to Eu^{3+} in silica xerogels. J. Lumin. 2014. V. 154. P. 290–293. doi.org/10.1016/j.jlumin.2014.05.004
9. Zak N., Szpikowska-Sroka B., Swinarew A.S. et al. Structural and optical properties of Eu^{3+}/Gd^{3+} ions in silica xerogels and powders obtained by sol-gel method. J. Mol. Struct. 2016. V. 1126. P. 29–36. doi.org/10.1016/j.molstruc.2016.03.095
10. Szpikowska-Sroka B., Pawlik N., Goryczka T. et al. Influence of silicate sol-gel host matrices and catalyst agents on the luminescent properties of Eu^{3+}/Gd^{3+} under different excitation wavelengths. RSC Adv. 2015. V. 5. № 120. P. 98773–98782. doi.org/10.1039/C5RA15562B
11. Pawlik N., Szpikowska-Sroka B., Sołtys M. et al. Optical properties of silica sol-gel materials singly- and doubly-doped with Eu^{3+} and Gd^{3+} ions. J. Rare Earths. 2016. V. 34. № 8. P. 786–795. doi.org/10.1016/S1002-0721(16)60095-9
12. Rocha L.A., Schiavon M.A., Ribeiro S.J.L. et al. Eu^{3+}-doped SiO_2–Gd_2O_3 prepared by the sol-gel process: structural and optical properties. J. Sol-Gel Sci. Technol. 2015. V. 76. № 2. P. 260–270. doi.org/10.1007/s10971-015-3773-6
13. Stone B.T., Costa V.C., Bray K.L. In situ dehydroxylation in Eu^{3+}-doped sol-gel silica. Chem. Mater. 1997. V. 9. № 11. P. 2592–2598. doi.org/10.1021/cm970265l
14. Sychov M., Syrkov A., Nakanishi Y. et al. Acid-base aspect of control of nanocomposite electrical properties. In: Nanoscale-Arranged Systems for Nanotechnology / Ed. K.L. Levine. New York: Nova Publishers, 2015. P. 89–98.
15. Gun'ko V.M., Myronyuk I.F., Zarko V.I. et al. Morphology and surface properties of fumed silicas. J. Colloid Interface Sci. 2005. V. 289. № 2. P. 427–445. doi.org/10.1016/j.jcis.2005.05.051
16. Gun'ko V.M., Zarko V.I., Leboda R. et al. Aqueous suspension of fumed oxides: particle size distribution and zeta potential. Adv. Colloid Interface Sci. 2001. V. 91. № 1. P. 1–112. doi.org/10.1016/S0001-8686(99)00026-3
17. Lyu R., Zhang C., Xia T. et al. Efficient adsorption of methylene blue by mesoporous silica prepared using sol-gel method employing hydroxyethyl cellulose as a

template. Colloids Surf. A: Physicochem. Eng. Aspects. 2020. V. 606. Article 125425. doi.org/10.1016/j.colsurfa.2020.125425
18. Niftaliev S.I., Kuznetsova I.V., Tran Nhat Anh. The synthesis of the system SiO_2–Gd_2O_3–Eu_2O_3 and research on the acid-base properties and kinetics of particle formation in this system. Mater. Proc. 2025. V. 21. № 1. Article 2. doi.org/10.3390/materproc2025021002
19. Aliyeva N.M., Mammadov E.E., Qasimova F.İ., Qasimova L. Kh., İsmailov E.H., Taghiyeva Sh. F. Electron-acceptor centres in Fe-Zr/Al oxide catalysts and their participation in the conversion of ethanol into hydrocarbons. 2016. №1. P.60-64.
20. Bayramov M.R., Mehdiyeva G.M., Agayeva M.A., Hasanova G.M. Study of the corrosion inhibitors properties of water-soluble nitrogen consisting alkenylphenols derivatives. Azerbaijan Chemical Journal. 2020. №. 3. P. 71-75.
21. Yagubov A.I., Nuriyev A.N., Muradova N.M., Aliyeva S.A., Efendiyeva N.G. The sorbtion of methylene blue on the termal activation bentonite. Azerbaijan Chemical Journal. 2014. №3. P. 53-56
22. Fneich H., Gaumer N., Chaussedent S. et al. Europium-doped sol-gel SiO_2-based glasses: effect of the europium source and content, magnesium addition and thermal treatment on their photoluminescence properties. Molecules. 2018. V. 23. № 7. Article 1768. doi.org/10.3390/molecules23071768
23. Ulfa M., Prasetyoko D., Trisunaryanti W. et al. The effect of gelatin as pore expander in green synthesis mesoporous silica for methylene blue adsorption. Sci. Rep. 2022. V. 12. Article 15271. doi.org/10.1038/s41598-022-19615-5
24. Niftaliev S.I., Kuznetsova I.V., Saranov I.A. et al. Synthesis of nanosized gadolinium oxide. Glass Phys. Chem. 2019. V. 45. P. 232–237.
25. GOST 4453–74. Active charcoal, wood-based, powdered [Electronic resource]. URL: http://gostexpert.ru/gost/gost-4453-74 [in Russian].
26. Arefieva O.D., Pirogovskaya P.D., Panasenko A.Y. et al. The acid-base properties of amorphous silica from straw and rice husk. Khimiya Rastitel'nogo Syr'ya. 2021. № 1. P. 327–335. [in Russian]
27. Dondur V., Fidler D., Adnadjević B. et al. The kinetics of water desorption from porous glasses. J. Therm. Anal. 1987. V. 32. P. 613–622. doi.org/10.1007/BF01912714
28. Lian M., Chen J., Yang X. et al. Preparation and luminescent properties of Eu^{3+} doped Gd_2O_3–SiO_2 nanocomposites. Cailiao Kexue [in Chinese]. 2019. V. 9. № 3. P. 280–288. doi.org/10.12677/MS.2019.93037
29. Meza O., Villabona-Leal E.G., Diaz-Torres L.A. et al. Luminescence concentration quenching mechanism in Gd_2O_3:Eu^{3+}. J. Phys. Chem. A. 2014. V. 118. № 8. P. 1390–1396. doi.org/10.1021/jp4119502
30. Charczuk N., Targońska S., Zákutná D. et al. Europium(III) and gadolinium(III) co-doped nanohydroxyapatite with enhanced photoluminescence as potential multimodal bioimaging agent. Ceram. Int. 2024. V. 50. № 9. P. 14601–14613. doi.org/10.1016/j.ceramint.2024.01.372
31. Trejo-García P., Palomino-Merino R., De la Cruz J. et al. Luminescent properties of titania doped with nanoparticles of gadolinium oxide and europium. Ceram. Int. 2020. V. 46. № 16. P. 26326–26334. doi.org/10.1016/j.ceramint.2020.06.086
32. Szpikowska-Sroka B., Żak N., Pisarski W.A. Influence of Gd^{3+} concentration on luminescence properties of Eu^{3+} ions in sol-gel materials. J. Mol. Struct. 2016. V. 1126. P. 259–264. doi.org/10.1016/j.molstruc.2016.01.083
33. Saranov I.A., Niftaliev S.I., Toroptsev V.V. et al. Investigation of the quality of water in the process of its purification using ultrafiltration by the method of differential scanning calorimetry. Vestnik Voronezhskogo Gosudarstvennogo Universiteta Inzhenernykh Tekhnologii [in Russian]. 2021. V. 83. № 87. P. 323–329.
34. Lishai N.V., Savitskaya T.A., Tsyhankova N.G. et al. Research of the adsorption of methylene blue by enterosorbents of various nature. Zhurnal Belorusskogo Gosudarstvennogo Universiteta. Khimiya [in Russian]. 2021. № 1. P. 58–74. doi.org/10.33581/2520-257X-2021-1-58-74
35. Barros J.M.F. et al. Hydrothermal Synthesis and Properties of Nanostructured Silica Containing Lanthanide Type Ln–SiO_2 (Ln = La, Ce, Pr, Nd, Eu, Gd, Dy, Yb, Lu). Nanomaterials. 2023. V. 13. Article 382. DOI: 10.3390/nano13030382.

SiO_2–Gd_2O_3–Eu_2O_3 SİSTEMLƏRİNİN SİNTEZİ VƏ SƏTHİ XASSƏLƏRİNİN TƏDQİQİ

Niftəliyev S. İ., Kuznetsova İ.V., Tran Nhat Anh, Çıraqov F.M.

Üçkomponentli SiO_2–Gd_2O_3–Eu_2O_3 sistemi sol–gel üsulu ilə sulu mühitdə tetraetoksisilanın (TEOS) hidrolizi nəticəsində sintez edilmişdir. Termiki analiz göstərmişdir ki, gelin dehidratlaşması əsasən aşağı temperatur sahəsində baş verir və fiziki adsorbsiya olunmuş, eləcə də zəif bağlı suyun uzaqlaşdırılması ilə əlaqədardır. Üçkomponentli gellər üçün görünən aktivləşmə enerjisi 30–34 kC/mol, SiO_2 geli üçün isə təxminən 40 kC/mol təşkil etmişdir ki, bu da suyun əsasən fiziki xarakterli bağlanmasını göstərir. Kalsinasiya olunmuş nümunələr Eu^{3+} ionlarına xas qırmızı lüminessensiya nümayiş etdirmişdir; ən intensiv zolaq 612 nm-də müşahidə olunmuş və $^5D_0 \rightarrow {}^7F_2$ keçidinə uyğun gəlmişdir. Maksimal lüminessensiya intensivliyi 1000 °C-də kalsinasiya olunmuş SiO_2–Gd_2O_3–Eu_2O_3 = 92:5:3 tərkibli nümunədə əldə edilmişdir, nadir torpaq oksidlərinin miqdarının daha da artırılması isə konsentrasiya sönməsinə səbəb olmuşdur. Optimal həyəcanlandırma dalğa uzunluğu 393 nm olmuşdur. Eyni 92:5:3 tərkibli, 700 °C-də kalsinasiya olunmuş nümunə metilen mavisinə görə ən yüksək adsorbsiya tutumuna — 108,32 mq/q — malik olmuş, bu göstərici 1000 °C-də kalsinasiyadan sonra 79,08 mq/q-a qədər azalmışdır. Alınmış nəticələr göstərir ki, SiO_2–Gd_2O_3–Eu_2O_3 materiallarının lüminessensiya və adsorbsiya xassələri tərkibin, kalsinasiya temperaturunun və səthin turşu–əsas vəziyyətinin idarə olunması ilə tənzimlənə bilər.

Açar sözlər: *SiO_2–Gd_2O_3–Eu_2O_3 sol–gel sintezi; tetraetoksisilan; europium lüminessensiyası; metilen mavisinin adsorbsiyası; səthin turşu–əsas xassələri.*